

# Method for Adjusting Single Matching Network for High-Power Transfer Efficiency of Wireless Power Transfer System

Dong-Wook Seo, Jae-Ho Lee, and Hyungsoo Lee

A wireless power transfer (WPT) system is generally designed with the optimum source and load impedance in order to achieve the maximum power transfer efficiency (PTE) at a specific coupling coefficient. Empirically or intuitively, however, it is well known that a high PTE can be attained by adjusting either the source or load impedance. In this paper, we estimate the maximum achievable PTE of WPT systems with the given load impedance, and propose the condition of source impedance for the maximum PTE. This condition can be reciprocally applied to the load impedance of a WPT system with the given source impedance. First, we review the transducer power gain of a two-port network as the PTE of the WPT system. Next, we derive two candidate conditions, the critical coupling and the optimum conditions, from the transducer power gain. Finally, we compare the two conditions carefully, and the results therefore indicate that the optimum condition is more suitable for a highly efficient WPT system with a given load impedance.

**Keywords:** Matching network, Power gain, Power transfer efficiency, Transducer power gain, Two-coil WPT system, Two-port network, Z-parameter.

## I. Introduction

Recent interest in wireless power transfer (WPT) systems, particularly their potential applications in implants [1], [2] and high-power demanding devices [3], [4], has fueled the growth of related researches. Most researches related to WPT systems have focused on estimating the maximum power transfer efficiency (PTE) and deriving the optimum load and source to achieve the maximum PTE [5]–[10]. Nowadays, apart from two- and four-coil WPT systems, a WPT system equipped with an increased number of coils has been studied to lengthen the transmission distance or improve the PTE [11]. Changing the operating frequency as well as the resonance frequencies of the resonators has also been studied to improve the PTE [12]–[14]. Further, the scope of studies on the WPT system has been extended from the inductive link to the various propagation links such as ultrasound, conduction, and optic links [15]–[17].

Studies on WPT systems using inductive coupling have employed a variety of methods such as a coupled mode method [5], an equivalent circuit model [6]–[9], and a spherical mode method [10]. However, they have shown the same results: an optimum source, an optimum load, and the maximum PTE. In [18], our group modeled a two-coil WPT system on a two-port network, and derived the operating and transducer power gains using the Z-parameters of the two-port network. We considered the transducer power gain as the PTE of the WPT system, and used the operating power gain and conjugate matching condition to obtain the optimum load and source condition. We confirmed that the WPT system with the optimum source and load could achieve the maximum PTE at

Manuscript received Nov. 20, 2015; revised June 30, 2016; accepted Aug. 17, 2016.

Dong-Wook Seo (seodongwook@etri.re.kr), Jae-Ho Lee (corresponding author, jhlee1229@etri.re.kr), and Hyungsoo Lee (hsulee@etri.re.kr) are with the Daegu-Gyeongbuk Research Center, ETRI, Daegu, Rep. of Korea.

the target-coupling coefficient by substituting the optimum condition into the transducer power gain. In addition, the operating power gain has the maximally achievable value at the target-coupling coefficient and even higher values beyond it. These results indicate that a high PTE can be achieved even under the changing operating environment of a WPT system by adjusting only the source impedance for the given load impedance.

Most receiving devices are generally required to be small and simple, and it is therefore not favorable to arbitrarily change the load impedance of the device. Achieving a high PTE by adjusting only the source impedance will be beneficial to the control of the PTE. However, there is little information available on how the source impedance should be adjusted for the given load impedance.

In this paper, we derive the critical coupling condition at which the WPT has the maximum PTE without a frequency splitting from the transducer power gain of a two-port network. We show that the critical coupling condition places the WPT system into a critical coupled state by adjusting only the source impedance for the given load impedance. In addition, we derive the optimum condition for the maximum PTE from the transducer power gain. This optimum condition involves not only the optimum source and load but also the optimum source under the given load. For the given load, we compare the results of the critical coupling condition with those of the optimum condition.

The remainder of this paper is organized as follows. In Section II, we briefly define the employed notations and review the characteristics of the operating and transducer power gains of a two-coil WPT system. In Section III, the critical coupling and optimum conditions are then evaluated from the transducer power gain. The analytical and simulated results are addressed in Section IV. Finally, this paper ends in Section V with some concluding remarks and a summary of the present work.

## II. Review of PTE of WPT System

General two-coil resonant WPT systems can be simply represented as shown in Fig. 1(a), and can also be replaced with a terminated T-equivalent two-port network with an input source using the Z-parameters in Fig. 1(b). Because the power gain of a two-port network is defined as the ratio of output power to input power, we can obtain the PTE of the two-coil WPT system by estimating the power gain of the two-port network. Among some of the defined power gains, the operating power gain  $G_p$  and transducer power gain  $G_T$  are given by [18]

$$G_p = \left| \frac{Z_{12}}{Z_{22} + Z_L} \right|^2 \frac{\text{Re}\{Z_L\}}{\text{Re}\{Z_{in}\}} \quad \text{and} \quad (1)$$

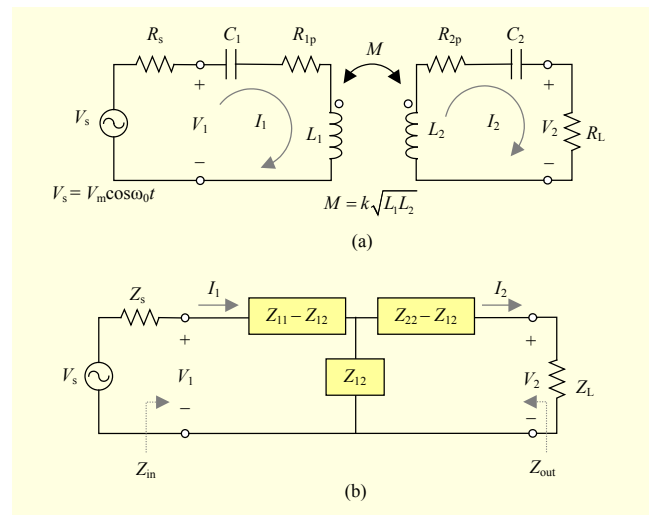


Fig. 1. Equivalent circuit model: (a) simplified two-coil WPT system and (b) terminated T-equivalent two-port network with input source using Z-parameters.

$$G_T = \frac{4 \text{Re}\{Z_s\} \text{Re}\{Z_L\} |Z_{21}|^2}{|(Z_{11} + Z_s)(Z_{22} + Z_L) - Z_{12}Z_{21}|^2}, \quad (2)$$

where  $Z_{11}$  and  $Z_{22}$  are  $R_{1p} + j\omega L_1 + 1/j\omega C_1$  and  $R_{2p} + j\omega L_2 + 1/j\omega C_2$ , respectively. Both  $Z_{12}$  and  $Z_{21}$  are  $j\omega M$ . The operating power gain is dependent on the load impedance,  $R_L$ , whereas the transducer power gain is dependent on both the source impedance and the load impedance. In other words, the operating power gain indicates the maximum achievable PTE using a two-port network and the load impedance regardless of the source impedance, whereas the transducer power gain indicates the PTE using a two-port network, source impedance, and load impedance.

In a previous study of [18], the optimum load of (3) was derived by partially differentiating the operating power gain with respect to the load impedance, and formulating the maximum achievable PTE of (4) at a specific coupling coefficient under the condition of (3). From the conjugate matching condition, we obtained the optimum source of (5). The source and load can be transformed into the optimum values by the matching networks, as shown in Fig. 2. If the matching networks are implemented by lumped elements, the WPT system has a two-coil structure. On the contrary, if the matching networks are implemented by the air-core transformers, the WPT system has a four-coil structure.

$$Z_{L,\text{opt}} = Z_{\text{out}}^* = R_{2p} \sqrt{1 + k^2 Q_{1u} Q_{2u}} - j\omega L_2, \quad (3)$$

$$\eta_{\text{max}} = \frac{\Delta}{(1 + \sqrt{1 + \Delta})^2} \Bigg|_{\Delta = k^2 Q_{1u} Q_{2u}}, \quad \text{and} \quad (4)$$

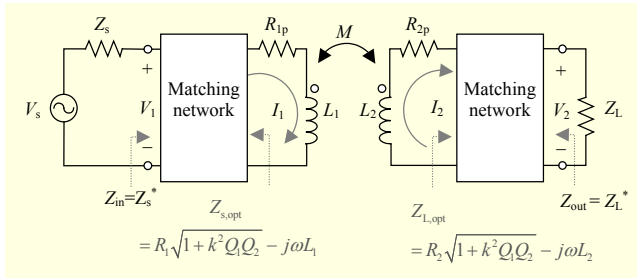


Fig. 2. Equivalent circuit model of two-coil WPT system using input-and output-matching networks.

$$Z_{s,opt} = Z_{in}^* = R_{1p} \sqrt{1 + k^2 Q_{1u} Q_{2u}} - j\omega L_1, \quad (5)$$

where  $Q_{1u} = \omega_0 L_1 / R_{1p}$  and  $Q_{2u} = \omega_0 L_2 / R_{2p}$  are the unloaded Q-factor of the primary and secondary coils, respectively. Because (3) and (5) are functions of the coupling coefficient  $k$ , (4) indicates the achievable maximum PTE at the specific coupling coefficient of the WPT system equipped with the optimum load and the source of (3) and (5); the specific coupling coefficient is called the target-coupling coefficient throughout this paper.

Consider the relationship among the operating power gain, transducer power gain, and maximum PTE. First, assume a two-coil WPT system with the parameters listed in Table I, which are identical to those used in [13]. To obtain the maximum PTE at the target-coupling coefficient of 0.0125, the source and load impedance should be  $15.74 - j1.256 \times 10^3 \Omega$  from (3) and (5). Next, the input and output matching networks were designed to transform the source and load impedance of 50 ohm to the optimum impedances. The designed WPT system is simulated using Keysight's Advanced Design System (ADS), and the Z-parameters of the two-coil WPT system are then obtained. The operating and transducer power gains are estimated by substituting the Z-parameters into (1) and (2), and are plotted in Fig. 3. The solid line represents the maximum PTE of (4) as a function of the coupling coefficient. At the target-coupling coefficient of 0.0125, both the operating and transducer power gains attain the maximum PTE. The transducer power gain decreases dramatically as the coupling coefficient deviates from the target-coupling coefficient. In other words, the optimum source and load are concurrently satisfied to have the maximum PTE at the target-coupling coefficient, and they do not guarantee a high PTE beyond the target-coupling coefficient. On the other hand, the operating power gain does not have the maximum PTE beyond the target-coupling coefficient, but still has a higher PTE than the PTE at the target-coupling coefficient. This means that a high PTE can be achieved by adjusting only the source impedance, without varying the load impedance. This work deals mainly with how a high PTE can be achieved by adjusting only the

Table 1. Circuit values used to evaluate the simplified model.

Parameters	Value	Description
$L_1, L_2$	20 $\mu$ H	Inductance of primary and secondary coils
$R_{1p}, R_{2p}$	1 $\Omega$	Parasitic resistance of primary and secondary coils
$Z_s, Z_L$	50 $\Omega$	Source and load impedance
$k$	0.0125	Target coupling coefficient
$f_0$	10 MHz	Operating frequency

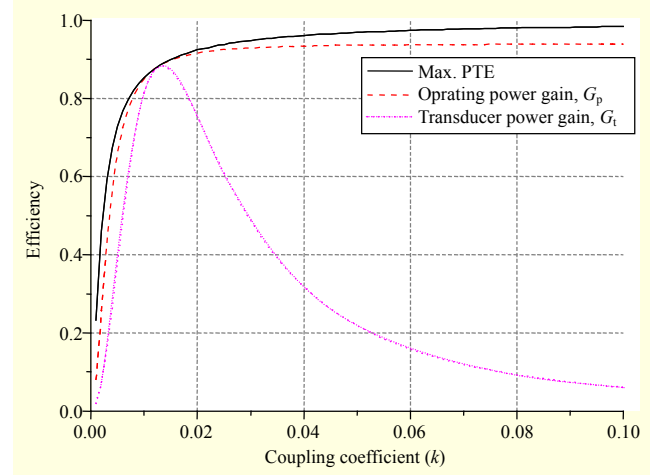


Fig. 3. Achievable maximum PTE, and the operating and transducer power gains at an operating frequency of 10 MHz with respect to the coupling coefficient.

source impedance at the non-target-coupling coefficient.

### III. Critical Coupling and Optimum Conditions for High PTE

To achieve a high PTE, we consider two candidate conditions: critical coupling and optimum conditions. Under the former condition, the WPT system transfers power into the load at the operating frequency without frequency splitting. The latter condition is obtained such that the partial differentiation of the transducer power gain with respect to the source resistance is zero at the operating frequency.

#### 1. Critical Coupling and its Condition for High PTE

It is a well-known fact that when the coupling coefficient passes over a specific value, the critical coupling state enters into an over-coupled state and a frequency splitting occurs. Because the frequency splitting transfers the power into the load, not through the operating frequency but through the split

frequencies, the PTE at the operating frequency decreases [6], [20]. Therefore, the critical coupling guarantees a high PTE.

The relationship between the frequency splitting and PTE can be ascertained by using an analytically expressed PTE, and is as follows:

$$\eta = \frac{4R_s}{R_L} \cdot \left| \frac{j\omega k \sqrt{L_1 L_2} R_L}{Z_1 Z_2 + \omega^2 k^2 L_1 L_2} \right|^2, \quad (6)$$

where  $Z_1$  and  $Z_2$  are the total series impedance of the primary and secondary resonators, respectively. A derivation of (6) is summarized in the Appendix.

Applying the parameters of Table 1 to the system, the series capacitances of  $C_1$  and  $C_2$  are 1.27 nF in common to resonate at the operating frequency. The resistances of the source and load are required to be 15.74  $\Omega$  from (3) and (5) to maximize the PTE at the target-coupling coefficient of 0.0125. Through the mentioned values and parameters, the PTE is calculated using (6) within an operating frequency range of 5 MHz to 15 MHz and a coupling coefficient range of 0.001 to 0.1, as shown in Fig. 4. The WPT system reaches the maximum PTE of 0.88 at an operating frequency of 10 MHz and target-coupling coefficient of 0.0125. When the coupling coefficient goes beyond the target-coupling coefficient, the PTE has peak values at two frequencies near the operating frequency (10 MHz) but not at the operating frequency. At the critical coupling coefficient, however, it is worth noting that the PTE of the WPT system with the fixed operating frequency is maximized.

To find the critical coupling condition, consider the transducer power gain at the operating frequency. Because the resonators have only resistance components at the operating frequency, (2) becomes

$$G_T|_{\omega=\omega_0} = \frac{4R_s R_L \cdot \omega_0^2 k^2 L_1 L_2}{((R_{1p} + R_s)(R_{2p} + R_L) + \omega_0^2 k^2 L_1 L_2)^2} \quad (7)$$

$$= \frac{4R_s R_L}{R_1 R_2} \cdot \frac{k^2 Q_1 Q_2}{(1 + k^2 Q_1 Q_2)^2},$$

where  $R_1$  and  $R_2$  are the total resistance of the primary and secondary resonators,  $R_1 = R_s + R_{1p}$  and  $R_2 = R_L + R_{2p}$ , respectively. In addition,  $Q_1$  and  $Q_2$  are the loaded Q-factor of the primary and secondary coils,  $Q_1 = \omega_0 L_1 / R_1$  and  $Q_2 = \omega_0 L_2 / R_2$ .

Because the transducer power gain at the operating frequency has the maximum value at the critical coupling coefficient, the derivative of (7) at the critical coupling coefficient is zero. Therefore, the critical coupling coefficient is obtained by

$$\frac{\partial G_T|_{\omega=\omega_0}}{\partial k} = 0 \rightarrow k_{\text{critical}} = \frac{1}{\sqrt{Q_1 Q_2}}. \quad (8)$$

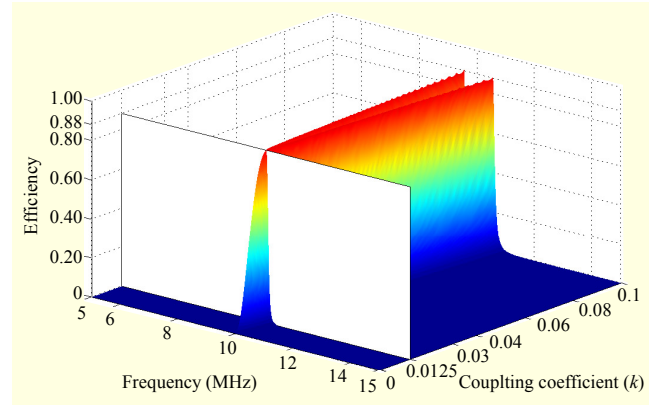


Fig. 4. Operating and transducer power gains at an operating frequency of 10 MHz with respect to the coupling coefficient.

The critical coupling coefficient of (8) is identical to the result of previous studies [19], [20]. Equation (8) can be rewritten as

$$k_{\text{critical}}^2 = \frac{(R_{1p} + R_s)(R_{2p} + R_L)}{\omega_0^2 L_1 L_2}. \quad (9)$$

The coil parameters such as  $L_{1(2)}$  and  $R_{1p(2p)}$  are generally not changed, whereas the source and load impedance are variable depending on the state of the power generator or load and can be adjusted by the matching network. Therefore, we can obtain the critical coupling at a desired coupling coefficient from (9) by changing the source or load resistances.

Arranging (9) for  $R_s$  and  $R_L$ , we obtain

$$R_{s,\text{critical}}|_{\text{for given } R_L} = R_{1p}(k^2 Q_{1u} Q_{2u} - 1) \quad \text{and} \quad (10)$$

$$R_{L,\text{critical}}|_{\text{for given } R_s} = R_{2p}(k^2 Q_1 Q_{2u} - 1). \quad (11)$$

The variation of the WPT environment results in a change in the coupling coefficient, which can be adjusted to the critical coupling coefficient by transforming the source impedance into the value of (10) for the given load impedance. The transformation is conducted by manipulating the input-matching network. Reciprocally, if the load impedance is transformed into the value of (11) for the given source impedance, the WPT system enters a critical coupled state.

Assume that the source and load resistances have the same times as their parasitic resistances as follows:

$$R_s = a \cdot R_{1p}, \quad R_L = a \cdot R_{2p}. \quad (12)$$

The source and load resistances for critical coupling can be summarized by

$$R_{s,\text{critical}} = R_{1p} \left( \sqrt{k^2 Q_{1u} Q_{2u}} - 1 \right) \quad \text{and} \quad (13)$$

$$R_{L,\text{critical}} = R_{2p} \left( \sqrt{k^2 Q_{1u} Q_{2u}} - 1 \right). \quad (14)$$



Equations (13) and (14) are dissimilar from the real parts of (3) and (5). Furthermore, substituting (3) and (5) into (8), we obtain

$$k_{\text{critical}} = \frac{1}{\sqrt{Q_{1u}Q_{2u}}} + \sqrt{\frac{1}{Q_{1u}Q_{2u}} + k^2}. \quad (15)$$

From (15), it can be observed that the target-coupling coefficient  $k$  of the optimum condition is not identical to the critical coupling coefficient  $k_{\text{critical}}$ . This means that the critical coupling results in the maximum PTE at the operating frequency, but cannot lead to the maximum PTE that can be achieved with the optimum source and load for the target-coupling coefficient.

When the coils have a high unloaded Q-factor ( $Q_{1u}Q_{2u} \gg 1$ ), the critical coupling coefficient of (15) approaches the target-coupling coefficient. On the contrary, the LF-band coil has a comparatively low unloaded Q-factor ranging from 10 up to 200. Consequently, in the case of a loosely coupled LF-band system, the target-coupling coefficient is distinguished from the critical coupling coefficient.

## 2. Optimum Condition for High PTE

From (6), the transducer power gain is expressed as a function of the variables  $R_s$  and  $R_L$ . The PTE is calculated with respect to  $R_s$  and  $R_L$  at the operating frequency and target-coupling coefficient by applying the parameters of Table 1 to (6), as shown in Fig. 5. From the calculation results, the maximum PTE of 0.88 can be obtained only with the optimum source and load. On the other hand, even though the source and load resistances deviate from the optimum values, a reasonably high PTE is still achieved. Herein, we derive not only the optimum source and load for the maximum PTE but also the optimum source with a given load impedance for a high PTE from the transducer power gain.

Here,  $\partial G_T|_{\omega=\omega_0}/\partial R_s$  represent the rate of change of the PTE with respect to  $R_s$  when  $R_L$  is given. Hence, the value of  $R_s$ , for which  $\partial G_T|_{\omega=\omega_0}/\partial R_s = 0$ , corresponds to the maximum point of the transducer power gain. That is, the relation of (16) is obtained to achieve a high PTE of the WPT system for the given  $R_L$ . Similarly, the relation of (17) is derived to maximize the PTE for the given  $R_s$  from  $\partial G_T|_{\omega=\omega_0}/\partial R_L = 0$ .

$$(R_{1p} - R_s)(R_{2p} + R_L) + \omega_0^2 k^2 L_1 L_2 = 0, \quad (16)$$

$$(R_{1p} + R_s)(R_{2p} - R_L) + \omega_0^2 k^2 L_1 L_2 = 0. \quad (17)$$

Arranging (16) for  $R_s$ , we obtain

$$R_{s,\text{opt}}|_{\text{for given } R_L} = R_{1p} (1 + k^2 Q_{1u} Q_{2u}). \quad (18)$$

Similarly, we obtain  $R_L$  from (17) as follows:

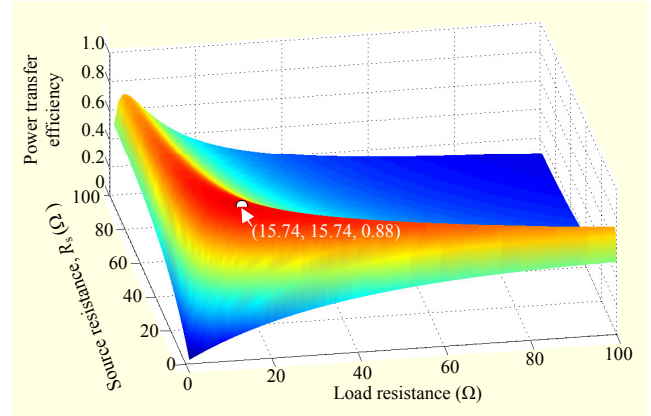


Fig. 5. Transducer power gains at an operating frequency of 10 MHz and a coupling coefficient of 0.0125 with respect to the source and load resistances.

$$R_{L,\text{opt}}|_{\text{for given } R_s} = R_{2p} (1 + k^2 Q_{1u} Q_{2u}). \quad (19)$$

Equation (18) is the optimum source resistance for the given load resistance; on the other hand, (19) is the optimum load resistance for the given source resistance.

Solving the simultaneous equations of (16) and (17) gives

$$R_{s,\text{opt}} = R_{1p} \sqrt{1 + k^2 Q_{1u} Q_{2u}} \quad \text{and} \quad (20)$$

$$R_{L,\text{opt}} = R_{2p} \sqrt{1 + k^2 Q_{1u} Q_{2u}}. \quad (21)$$

Equations (20) and (21) are identical to the real parts of (5) and (3), which are derived from the operating power gain and conjugate matching condition. It should be noted that (20) and (21) must be concurrently satisfied to achieve the maximum PTE.

## IV. Simulation Results and Discussions

This section addresses the critical coupling and optimum conditions described in Section II, which are demonstrated through a circuit simulation using Keysight's ADS and the analytical approach of (6).

Consider the WPT system using the parameters of Table 1. The optimum source and load resistances are 15.74  $\Omega$  from (18) and (19) for the target-coupling coefficient of 0.0125, and the source and load impedance for the critical coupling are 14.71  $\Omega$  from (13) and (14). On the other hand, to resonate at 10 MHz, the reactance of both the source and load is  $-j1.256 \times 10^3 \Omega$  under the critical coupling and optimum conditions. As shown in Fig. 6, the L-section input-matching network is used to transform the source impedance into the impedance looking into the input source,  $Z_s$ , of the optimum or critical coupled values. Similarly, the output-matching network is used to transform the load impedance into the impedance looking into

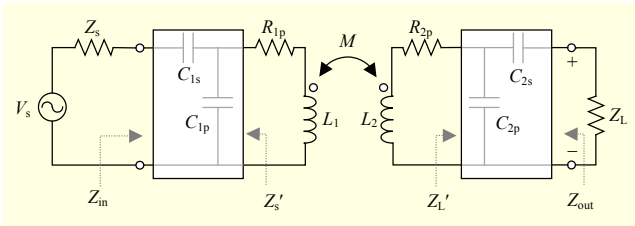


Fig. 6. Equivalent circuit model of two-coil WPT system using input- and output-matching networks having an L-section structure.

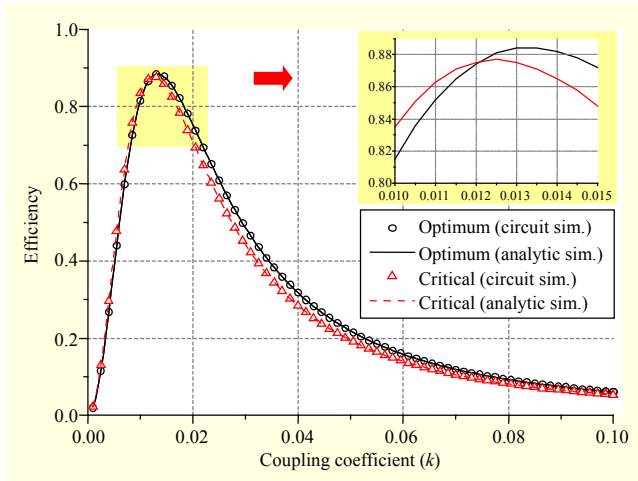


Fig. 7. PTEs based on the optimum and critical conditions for the target-coupling coefficient of 0.0125.

the load,  $Z_L$ , of the optimum or critical coupled values. The parameters of the matching networks (for  $k = 0.0125$ ) are summarized in Tables 2 and 3. Under the optimum and critical coupling conditions, the PTEs are plotted in Fig. 7 for the target-coupling coefficient of 0.0125. The circuit-simulated and analytical results are perfectly matched. The PTE under the critical coupling condition has a peak of 0.877 at the target-coupling coefficient, while the PTE under the optimum condition is 0.881 at the target-coupling coefficient and has a peak of 0.884 at the coupling coefficient of 0.013. These results reveal that the optimum condition causes the PTE to have a peak value at a slightly higher coupling coefficient than the target coupling and not at the target-coupling coefficient. Moreover, the optimum condition renders the PTE higher than that under the critical coupling condition at the target-coupling coefficient. In addition, as described in Tables 2 and 3, when the coupling coefficient is changed from 0.0125 to 0.0750, the source resistance should be within a range of 14.71  $\Omega$  to 564.49  $\Omega$  under the critical coupling condition, whereas the source resistance should be adjusted from 15.74  $\Omega$  to 531.63  $\Omega$  under the optimum condition. Therefore, the critical coupling condition is more sensitive to the changed coupling coefficient than the optimum condition.

Table 2. Critical coupling source and its L-section components with respect to the target-coupling coefficient for a fixed load.

coupling coefficient ( $k$ )	$R'_s$	$C_{1p}$	$C_{1s}$	$R'_L$	$C_{2p}$	$C_{2s}$
0.0125	14.71 $\Omega$	5.80 pF	6.87 pF	14.71 $\Omega$	5.80 pF	6.87 pF
0.0250	61.83 $\Omega$	178.5 $\mu$ H	14.08 pF			
0.0375	140.37 $\Omega$	29.7 $\mu$ H	21.14 pF			
0.0500	250.33 $\Omega$	16.3 $\mu$ H	27.90 pF			
0.0625	391.70 $\Omega$	11.5 $\mu$ H	34.04 pF			
0.0750	564.49 $\Omega$	9.0 $\mu$ H	39.11 pF			

Table 3. Optimum source and its L-section components with respect to the target-coupling coefficient for a fixed load.

coupling coefficient ( $k$ )	$R'_s$	$C_{1p}$	$C_{1s}$	$R'_L$	$C_{2p}$	$C_{2s}$
0.0125	15.74 $\Omega$	5.56 pF	7.11 pF	15.74 $\Omega$	5.56 pF	7.11 pF
0.0250	59.96 $\Omega$	210.4 $\mu$ H	13.87 pF			
0.0375	133.66 $\Omega$	31.6 $\mu$ H	20.63 pF			
0.0500	236.84 $\Omega$	17.2 $\mu$ H	27.19 pF			
0.0625	369.49 $\Omega$	12.0 $\mu$ H	33.21 pF			
0.0750	531.63 $\Omega$	9.4 $\mu$ H	38.31 pF			

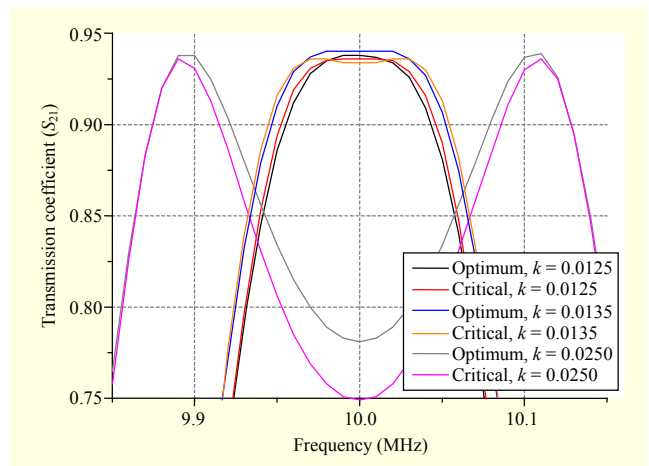


Fig. 8. Transmission coefficients of the two-port network with the optimum and critical conditions as a function of frequency for  $k = 0.0125, 0.0135,$  and  $0.0250$ .

Figure 8 shows the transmission coefficient,  $S_{21}$ , of the WPT system under the optimum and critical coupling conditions for several coupling coefficients. For  $k = 0.0125$ , the PTEs under the optimum and critical conditions have a single maximum value at an operation frequency of 10 MHz. However, the PTE under the optimum condition has a convex-shaped peak, whereas that under the critical condition has a flat-topped peak.

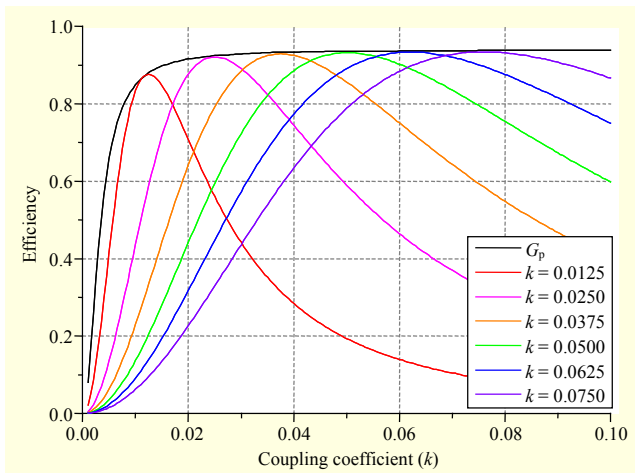


Fig. 9. Operating power gain and PTEs based on the critical condition for changed coupling coefficients of 0.0125, 0.0250, 0.0375, 0.0500, 0.0625, and 0.0750 when the load impedance is fixed.

For  $k = 0.0135$ , the frequency splitting occurs under the critical coupling condition, whereas the PTE under the optimum condition has a flat-topped peak without a frequency splitting. Additionally, the PTEs under both conditions have a frequency splitting for  $k = 0.0250$ . Obviously, the critical coupling condition creates the critical coupling at the target-coupling coefficient of 0.0125.

Assume that a WPT system fulfills the critical coupling condition at  $k = 0.0125$ , but that the coupling coefficient deviates from the target-coupling coefficient and the load impedance does not arbitrarily change. To satisfy the critical coupling condition for the changed coupling coefficient, the input-matching network transforms the source impedance into the critical source resistance obtained from (16). For the changed coupling coefficients, the critical source resistance and the corresponding parameters of the L-section matching network are summarized in Table 2.

Figure 9 shows the PTEs in substituting the source impedance with the critical source resistance for the changed target-coupling coefficients. Under the critical coupling conditions, the peaks of the PTEs are slightly less than the operating power gain. Figure 10 shows the transmission coefficients of the WPT system under the critical coupling condition with respect to the frequency for the changed target-coupling coefficients. Figure 10 shows that the system remains in a critical coupled state by adopting the critical coupling condition even for the changed target-coupling coefficients.

Suppose that a WPT system has the optimum source and load impedances at the target-coupling coefficient of 0.0125, but that the target-coupling coefficient is changed from 0.0125 to 0.0250, 0.0375, 0.0500, 0.0625, and 0.0750 owing to variations in the operating environment. Under the optimum

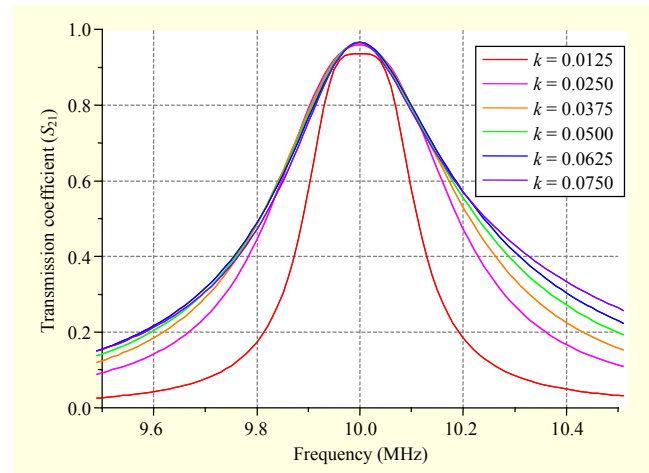


Fig. 10. Transmission coefficients of the two-port network under the critical coupling condition as a function of frequency for the changed target-coupling coefficients when the load impedance is fixed.

Table 4. Operating power and peaks of PTEs under the critical coupling and optimum conditions for the changed target-coupling coefficients.

Target-coupling coefficient	Operation power gain	Critical coupling condition	Optimum condition
0.0125	0.881	0.877	0.881
0.0250	0.925	0.921	0.925
0.0375	0.933	0.930	0.933
0.0500	0.936	0.932	0.936
0.0625	0.938	0.934	0.938
0.0750	0.939	0.934	0.938

condition, the input-matching network transforms the initial source resistance of (20) into the optimum source resistance from (18) for the given load impedance. For the optimum source impedance, the values of the lumped elements for the input-matching network are listed in Table 3. Figure 11 plots the PTEs of the WPT system with the optimum source resistance under the optimum condition. The plot indicates that the PTEs reach the operating power gain through only an adjustment of the source impedance for the optimum condition in spite of the changed target-coupling coefficients. For the changed target-coupling coefficients, the PTEs under the critical coupling and optimum conditions and the operating power gain are summarized in Table 4.

Adjusting only the source resistance obtained by the derived critical coupling and optimum conditions, the WPT system can have the critical coupling and maximum achievable PTE at the target-coupling coefficient, respectively. The critical coupling

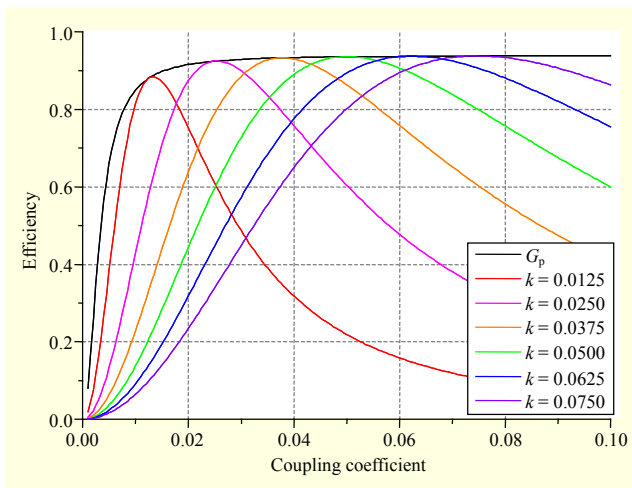


Fig. 11. Operating power gain and PTEs based on the optimum condition for the changed coupling coefficients of 0.0125, 0.0250, 0.0375, 0.0500, 0.0625, and 0.0750 when the load impedance is fixed.

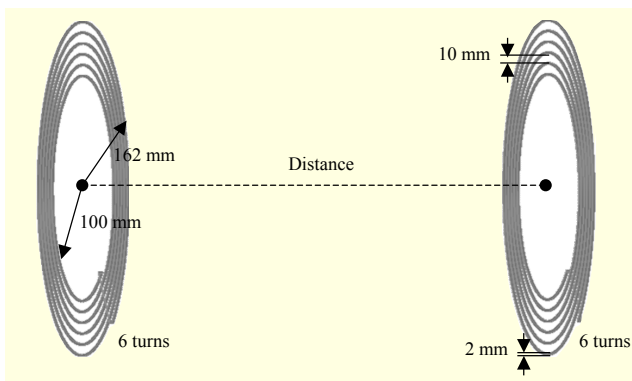


Fig. 12. Geometry of a four-coil WPT system for a 3D EM simulation.

and optimum conditions work well for a wide range of coupling coefficients.

To investigate the maximum available distance of the WPT system, the primary and secondary coils having the coil parameters listed in Table 1 should be modeled, and the coupling coefficient should be estimated with respect to the distance between the coils. Using an Ansys high-frequency structural simulator (HFSS), we modeled the coils as spiral coils with six turns, a line width of 2 mm, an outer radius of 162 mm, and a radius change of 10 mm, as shown in Fig. 12, and the relation between the coupling coefficient and the distance of the coils was then simulated and is illustrated in Fig. 13. Assume that the available distance is the maximum distance having a PTE of 50% or above, as in [5]. We can then estimate the available distance from Figs. 9, 11, and 13. In the case of the non-adjustable matching network, the WPT system with the optimum source and load impedance for the target-

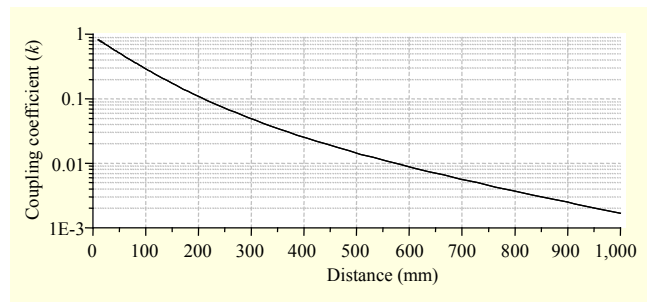


Fig. 13. Simulated coupling coefficient with respect to distance between the primary and secondary coils.

coupling coefficient of 0.0125 has an available distance of 370 mm to 685 mm, for a total of 315 mm, whereas the WPT system with the critical source and load impedance has an available distance of 387 mm to 697 mm, for a total of 310 mm. In the case of the adjustable input matching network, the available distance of the WPT system with the optimum and critical coupling conditions is the same distance of zero to 781 mm. These results reveal that the optimum condition provides a slightly better performance than the critical coupling condition in terms of the available distance and PTE.

## V. Conclusion

We regard a two-coil WPT system as a two-port network, and represent the PTE as the transducer power gain of a two-port network. From a comparison of the transducer power gain with the operating power gain, we found the potential to achieve a high PTE by adjusting only the source impedance when the coupling coefficient deviates from the target-coupling coefficient in a practical operating environment. An analytical method was applied to ascertain this possibility, and we also derived the critical coupling and optimum conditions from the transducer power gain. With the critical coupling and optimum conditions, the changed source impedance leads the system to achieve a high PTE. Under the proposed conditions, the WPT system was simulated using Keysight's ADS for the changed coupling coefficients. Consequently, under the critical coupling condition, the WPT system enters a critical coupled state, but achieves a PTE of slightly less than the optimum condition. The optimum condition yields the optimum source for the given load impedance as well as the optimum source and load impedances. Reciprocally, the condition also yields the optimum load for the given source impedance.

In a conventional WPT system, the source impedance has been empirically changed in an attempt to achieve a high PTE for the given load impedance. However, the proposed conditions provide an accurate achievable PTE and targeted source impedance for the given load impedance.



## VI. Appendix

Consider a two-coil series resonant WPT system, as shown in Fig. 1(a). The series impedance of the primary and secondary resonators can be written by

$$Z_1 = R_s + R_{1p} + j\omega L_1 + \frac{1}{j\omega C_1} \quad \text{and} \quad (\text{A.1})$$

$$Z_2 = R_L + R_{2p} + j\omega L_2 + \frac{1}{j\omega C_2}. \quad (\text{A.2})$$

Kirchhoff's voltage law for two resonant loops yields

$$I_1 Z_1 - j\omega M I_2 = V_s \quad \text{and} \quad (\text{A.3})$$

$$-I_2 Z_2 + j\omega M I_1 = 0. \quad (\text{A.4})$$

From (A.3), (A.4), and  $V_L = R_L \cdot I_2$ , the voltage gain will be

$$\frac{V_L}{V_s} = \frac{j\omega k \sqrt{L_1 L_2} R_L}{Z_1 Z_2 + \omega^2 k^2 L_1 L_2}. \quad (\text{A.5})$$

Because the transducer power gain may be regarded as the PTE, the PTE, which is the ratio of the power available from the source  $P_{avs}$  to the power delivered to the load  $P_L$ , is given by

$$\eta = G_T = \frac{P_L}{P_{avs}} = \frac{|V_L|^2 / 2R_L}{|V_s|^2 / 8R_s} = \frac{4R_s}{R_L} \left| \frac{V_L}{V_s} \right|^2. \quad (\text{A.6})$$

Equation (A.6) is identical to the square of  $|S_{21}|$  in [2]. Finally, substituting (A.5) into (A.6) yields

$$\eta = \frac{4R_s}{R_L} \cdot \left| \frac{j\omega k \sqrt{L_1 L_2} R_L}{Z_1 Z_2 + \omega^2 k^2 L_1 L_2} \right|^2. \quad (\text{A.7})$$

## References

- [1] D.W. Seo et al., "Open-Loop Self-Adaptive Wireless Power Transfer System for Medical Implant," *Microw. Opt. Technol. Lett.*, vol. 58, no. 6, June 2016, pp. 1271–1275.
- [2] D.-W. Seo, J.-H. Lee, and H. Lee, "Integration of Resonant Coil for Wireless Power Transfer and Implantable Antenna for Signal Transfer," *Int. J. Antennas Propag.*, Aug. 2016, pp. 7101207-1–7101207-7.
- [3] W. Zhang and C.C. Mi, "Compensation Topologies of High-Power Wireless Power Transfer Systems," *IEEE Trans. Veh. Technol.*, vol. 65, no. 6, June 2016, pp. 4768–4778.
- [4] J.M. Miller and A. Daga, "Elements of Wireless Power Transfer Essential to High Power Charging of Heavy Duty Vehicles," *IEEE Trans. Transport. Electrification*, vol. 1, no. 1, June 2015, pp. 26–39.
- [5] A. Karalis, J.D. Joannopoulos, and M. Soljačić, "Efficient Wireless Non-radiative Mid-range Energy Transfer," *Ann. Physics*, vol. 323, no. 1, Jan. 2008, pp. 34–48.
- [6] A.P. Sample, D.A. Meyer, and J.R. Smith, "Analysis, Experimental Results, and Range Adaption of Magnetically Coupled Resonators for Wireless Power Transfer," *IEEE Trans. Ind. Electron.*, vol. 58, no. 2, Feb. 2011, pp. 544–554.
- [7] S. Cheon et al., "Wireless Energy Transfer System with Multiple Coils via Coupled Magnetic Resonances," *ETRI J.*, vol. 34, no. 4, Aug. 2012, pp. 527–535.
- [8] K. Lee and D.-H. Cho, "Diversity Analysis of Multiple Transmitters in Wireless Power Transfer System," *IEEE Trans. Magn.*, vol. 49, no. 6, June 2013, pp. 2946–2952.
- [9] K. Lee and D.-H. Cho, "Simultaneous Information and Power Transfer Using Magnetic Resonance," *ETRI J.*, vol. 36, no. 5, Oct. 2014, pp. 808–818.
- [10] J. Lee and S. Nam, "Fundamental Aspects of Near-Field Coupling Small Antennas for Wireless Power Transfer," *IEEE Trans. Antennas Propag.*, vol. 58, no. 11, Nov. 2010, pp. 3442–3449.
- [11] M. Kiani and M. Ghovanloo, "A Figure-of-Merit for Designing High Performance Inductive Power Transmission Link," *IEEE Trans. Ind. Electron.*, vol. 60, no. 11, Nov. 2013, pp. 5292–5305.
- [12] D. Ahn, M. Kiani, and M. Ghovanloo, "Enhanced Wireless Power Transmission Using Strong Paramagnetic Response," *IEEE Trans. Magn.*, vol. 50, no. 3, Mar. 2014.
- [13] D.-W. Seo, J.-H. Lee, and H.-S. Lee, "Optimum Coupling to Achieve Maximum Output Power in a WPT System," *IEEE Trans. Power Electron.*, vol. 31, no. 6, June 2016, pp. 3994–3998.
- [14] R. Huang et al., "Frequency Splitting Phenomena of Magnetic Resonant Coupling Wireless Power Transfer," *IEEE Trans. Magn.*, vol. 50, no. 11, Nov. 2014.
- [15] M.G.L. Rose et al., "Acoustic Energy Transfer: A Review," *IEEE Trans. Ind. Electron.*, vol. 60, no. 1, Jan. 2013, pp. 242–248.
- [16] J. Dai and D.C. Ludoi, "A Survey of Wireless Power Transfer and a Critical Comparison of Inductive and Capacitive Coupling for Small Gap Applications," *IEEE Trans. Power Electron.*, vol. 30, no. 11, Nov. 2015, pp. 6017–6029.
- [17] S.D. Jarvis et al., "Development and Characterisation of Laser Power Converters for Optical Power Transfer Applications," *IET Optoelectron.*, vol. 8, no. 2, Apr. 2014, pp. 64–70.
- [18] D.-W. Seo, J.-H. Lee, and H. Lee, "Study on Two-Coil and Four-Coil Wireless Power Transfer Systems Using Z-parameter Approach," *ETRI J.*, vol. 38, no. 3, June 2016, pp. 568–578.
- [19] D. Ahn and S. Hong, "A Study on Magnetic Field Repeater in Wireless Power Transfer," *IEEE Trans. Ind. Electron.*, vol. 60, no. 1, Jan. 2012, pp. 360–371.
- [20] R. Huang et al., "Frequency Splitting Phenomena of Magnetic Resonant Coupling Wireless Power Transfer," *IEEE Trans. Magn.*, vol. 50, no. 11, Nov. 2014.



**Dong-Wook Seo** received his BS degree in electrical engineering from Kyungpook National University, Daegu, Rep. of Korea in 2003, and his MS degree and PhD in electrical engineering from Korea Advanced Institute of Science and Technology, Daejeon, Rep. of Korea in 2005 and 2011, respectively. He was a senior

researcher at the Defense Agency for Technology and Quality, Daegu, Rep. of Korea from 2011 to 2012. Since 2012, he has been a senior researcher with ETRI, Daegu, Rep. of Korea. His current research interests include numerical techniques in the area of electromagnetics, radar cross-section analysis, wireless power transfer, biomedical implantable devices, and automotive radar systems.



**Jae-Ho Lee** received his BS degree in electronic and electrical engineering from Kyungpook National University in 2002, and his MS degree in electrical and electronic engineering from the Korea Advanced Institute of Science and Technology in 2004. He received his PhD in electrical and electronic

engineering from Tokyo Institute of Technology, Japan in 2010. From 2004 to 2005, he worked at the Mobile Communication PM team of the Institute of Information and Technology Assessment, Daejeon, Rep. of Korea. He also worked for the Radar Research Center at Samsung Thales, Yongin, Rep. of Korea from 2010 to 2012. Since 2013, he has been a senior researcher with ETRI. His research interests include waveguide arrays, electromagnetic numerical analysis, biomedical implantable devices, automotive radar systems, and antennas.



**Hyungsoo Lee** received his BS degree in electrical engineering from Kyungpook National University, Daejeon, Rep. of Korea in 1980, and his PhD in IT engineering from Sungkyunkwan University, Suwon, Rep. of Korea in 1996. Since 1983, he has been a principal researcher with ETRI, Daejeon, Rep.

of Korea. His research interests include spectrum engineering, WPAN system designs, and biomedical IT convergence devices.